MicroRNA-433 Dampens Glucocorticoid Receptor Signaling, Impacting Circadian Rhythm and Osteoblastic Gene Expression*[S]

Spenser S. Smith, Neha S. Dole[1], Tiziana Franceschetti[2], Henry C. Hrdlicka, and Anne M. Delany[3]
From the Center for Molecular Medicine, UConn Health, Farmington, Connecticut 06030

Serum glucocorticoids play a critical role in synchronizing circadian rhythm in peripheral tissues, and multiple mechanisms regulate tissue sensitivity to glucocorticoids. In the skeleton, circadian rhythm helps coordinate bone formation and resorption. Circadian rhythm is regulated through transcriptional and post-transcriptional feedback loops that include microRNAs . How microRNAs regulate circadian rhythm in bone is unexplored. We show that in mouse calvaria, miR-433 displays robust circadian rhythm, peaking just after dark. In C3H/10T1/2 cells synchronized with a pulse of dexamethasone, inhibition of miR-433 using a tough decoy altered the period and amplitude of *Per2* gene expression, suggesting that miR-433 regulates rhythm. Although miR-433 does not directly target the *Per2* 3′-UTR, it does target two rhythmically expressed genes in calvaria, *Igf1* and *Hif1α*. miR-433 can target the glucocorticoid receptor; however, glucocorticoid receptor protein abundance was unaffected in miR-433 decoy cells. Rather, miR-433 inhibition dramatically enhanced glucocorticoid signaling due to increased nuclear receptor translocation, activating glucocorticoid receptor transcriptional targets. Last, in calvaria of transgenic mice expressing a miR-433 decoy in osteoblastic cells (Col3.6 promoter), the amplitude of *Per2* and *Bmal1* mRNA rhythm was increased, confirming that miR-433 regulates circadian rhythm. miR-433 was previously shown to target *Runx2*, and mRNA for *Runx2* and its downstream target, osteocalcin, were also increased in miR-433 decoy mouse calvaria. We hypothesize that miR-433 helps maintain circadian rhythm in osteoblasts by regulating sensitivity to glucocorticoid receptor signaling.

The circadian rhythm is an internal timing mechanism important for orchestrating physiological homeostasis, through synchronizing behavioral and physiological patterns. This coordinates biological processes critical for overall health, such as tissue repair and growth, maintenance of the immune response, and optimization of metabolism. The circadian rhythm is driven by a complex interaction between the hypothalamic suprachiasmatic nucleus (SCN),[4] also known as the central clock, and the peripheral circadian clocks. As the central oscillator, the SCN responds to environmental periodic cues, such as light, eating patterns, and temperature. In response to these cues, the SCN entrains peripheral circadian clocks through stimulation of neural or hormonal signals (*e.g.* glucocorticoids) to enact their effects on target tissues (1).

In the central oscillator and peripheral tissues, the rhythm is maintained locally by clock genes that interact through transcriptional and post-transcriptional feedback loops. The main positive regulators are aryl hydrocarbon receptor nuclear translocator-like (*Arntl* or *Bmal1*) and circadian locomotor output cycles kaput (*Clock*), which are negatively regulated by the period genes (*Per1*, *Per2*, and *Per3*) and the cryptochrome genes (*Cry1* and *Cry2*), among others (for a review, see Ref. 2). Bmal1 and Clock form a heterodimer and bind to E-box elements of target genes, including the *Per* and *Cry* genes, to rhythmically induce transcription. PER/CRY can negatively feedback to inhibit their own transcription as well as the transcription of *Bmal1*/*Clock*, ensuring the anti-phasic expression of clock proteins. This interaction between the clock proteins determines the oscillatory expression of target genes and contributes to the rhythmicity of physiological systems (3).

Bone is a continuously remodeling tissue, and disturbances in circadian rhythm have a negative impact on skeletal health (4–7). Bone remodeling is the coupled cycle of osteoclast-mediated bone resorption followed by osteoblast-mediated bone formation. This process is critical for renewal of bone in adults and for mineral homeostasis. Imbalance in the bone remodeling process can lead to prevalent diseases, such as osteoporosis.

In osteoblasts, 26% of genes display a diurnal expression pattern, including the master osteoblast transcription factor Runt-related transcriptional factor 2 (*Runx2*), bone morphogenetic protein 2 (*Bmp2*), osteocalcin (Oc, *Bglap*), insulin-like growth factor 1 (*Igf1*), and hypoxia-inducible factor 1α (*Hif1α*) (4, 6). Evidence suggests that, in humans, circadian rhythm coordinates bone remodeling so that it occurs primarily at night. For

[1] Present address: Dept. of Orthopedic Surgery, University of California San Francisco School of Medicine, San Francisco, CA 94143.
[2] Present address: Inst. of Medical Sciences, University of Aberdeen, Aberdeen AB25 2ZD, United Kingdom.
[3] To whom correspondence should be addressed: Center for Molecular Medicine, UConn Health, 263 Farmington Ave., Farmington, CT 06030. Tel.: 860-679-8730; Fax: 860-679-1258; E-mail: adelany@uchc.edu.

[4] The abbreviations used are: SCN, suprachiasmatic nucleus; miRNA, microRNA; ZT, Zeitgeber time; BMSC, bone marrow stromal cell; Dox, doxycycline; HDAC, histone deacetylase; GR, glucocorticoid receptor; GRE, glucocorticoid response element.

example, bone formation markers, such as serum osteocalcin, as well as serum markers of type I collagen synthesis, the major protein component of bone matrix, are highest in premenopausal women at night (7, 8). Moreover, serum levels of glucocorticoids, which are known to play an important role in synchronizing peripheral clocks, are critical for the diurnal variation in serum osteocalcin (9).

MicroRNAs (miRNAs) are key mediators of post-transcriptional regulation. These short (19–25-nucleotide) non-coding RNAs bind specific target mRNAs, resulting in mRNA degradation and/or translational suppression. Many miRNAs fine tune the timing and tempo of gene expression programs, and these post-transcriptional regulators are an important component of circadian clock control. Indeed, miRNAs display circadian rhythmicity in many tissues, including the liver, retina, and SCN (10, 11). miRNAs can directly regulate circadian clocks; for example, miR-191 directly targets the 3′-UTR of *Bmal1* in the liver (12). Alternatively, miRNAs can indirectly control circadian rhythm by targeting downstream regulators, as is the case for miR-122 targeting of nocturnin, a key circadian deadenylase (13). Conversely, clock genes can directly regulate miRNA expression; for example, BMAL1/CLOCK induces expression of miR-219, and *in vivo* miR-219 knockdown results in a lengthened circadian period (14).

miRNA regulation of circadian rhythm in the skeleton has not been reported. However, within the adrenal gland, miR-433 was recently shown to target the glucocorticoid receptor (GR; *Nr3c1*) 3′-UTR (15). Rhythmic secretion of glucocorticoids is critical for synchronizing local clocks in peripheral tissues, in part by activating transcription of *Per* genes (16). Moreover, as circulating glucocorticoid levels fluctuate diurnally, so does the sensitivity of tissues to glucocorticoids (17). Herein, we demonstrate that miR-433 regulates glucocorticoid signaling and impacts the expression of the circadian clocks and osteoblastic genes *in vitro* and *in vivo*.

Results

miR-433 Expression Is Rhythmic in Calvaria—To determine whether miR-433 might play a role in osteoblast circadian rhythm, we first determined whether it is under circadian regulation in the skeleton. RNA was isolated from calvaria of male mice kept under a 12-h light/dark cycle, represented as Zeitgeber time (ZT). ZT0 is the beginning of light exposure, whereas ZT12 is the beginning of light removal. Examining two markers of circadian rhythm, *Bmal1* and *Per2*, over two 24-h cycles, these two circadian genes displayed the expected anti-phasic pattern of expression throughout each 24-h cycle. For example, *Bmal1* mRNA expression was highest at ZT1, whereas *Per2* mRNA was low; the nadir for Bmal1 mRNA was just before light removal, whereas Per2 mRNA had its peak expression just after dark (Fig. 1A).

We analyzed the expression of three microRNAs, miR-433, miR-29a, and miR-30a, because they were either shown to display rhythmic expression in other tissues or were predicted via bioinformatics analysis to potentially target the glucocorticoid receptor or circadian clock genes (10). miR-433 displayed robust rhythmicity in mouse calvaria (Fig. 1B). The miR-433 expression pattern was anti-phasic in relation to *Bmal1* mRNA,
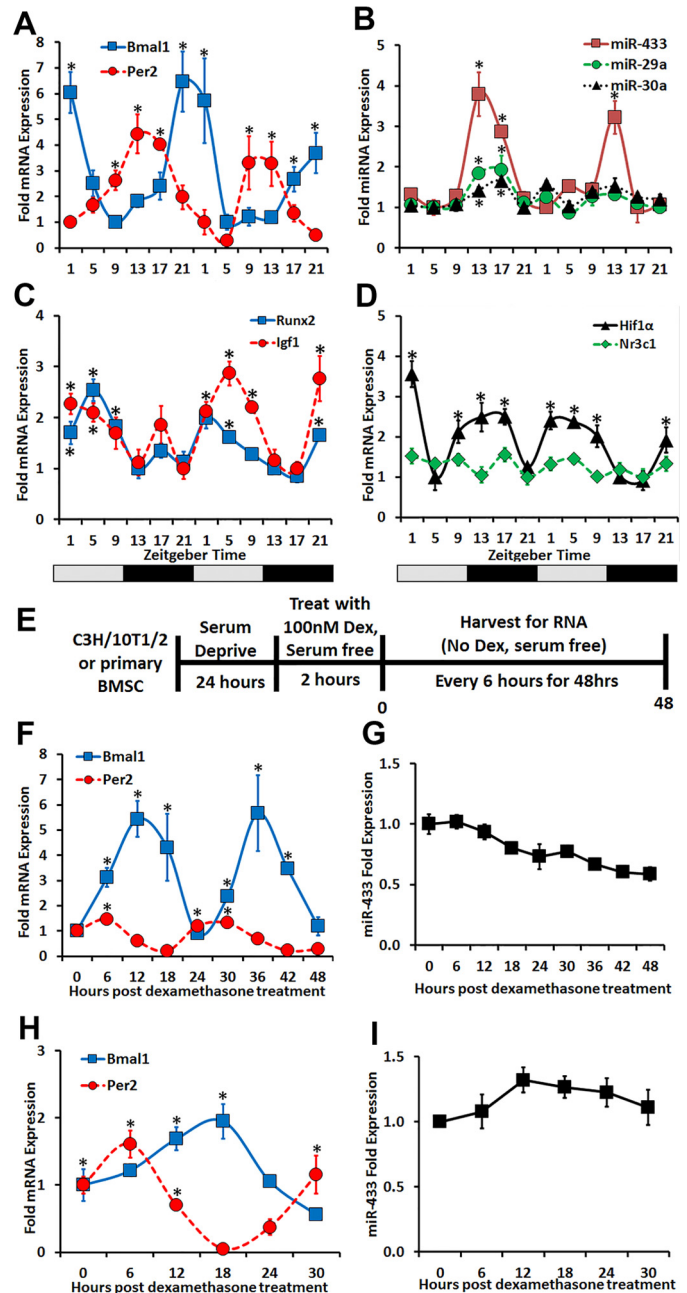

FIGURE 1. **Rhythmic expression of circadian clock mRNAs, miRNAs and osteogenic genes in mouse calvaria and validation of an *in vitro* model to study circadian rhythm.** C57BL/6J mice were kept under a 12-h light/dark cycle; calvaria were harvested every 4 h. Two 24-h cycles are shown. RNA levels were quantified by quantitative RT-PCR. ZT0 indicates the beginning of light exposure, and ZT12 indicates the beginning of light removal. *A*, markers of circadian rhythm, *Bmal1* (*blue*) and *Per2* (*red*). *B*, miR-433 (*red*), miR-29a (*green*), and miR-30a (*black*). *C* and *D*, osteogenic genes *Runx2* (*blue*) and *Igf1* (*red*) (*C*) and *Hif1α* (*black*) and *Nr3c1* (glucocorticoid receptor) (*green*) (*D*). -Fold change in each gene is expressed relative to the nadir (*n* = 5). *E*, experimental design for synchronizing C3H/10T1/2 cells and primary BMSCs. *F*–*I*, expression of *Bmal1* (*blue*) and *Per2* (*red*) mRNA and miR-433 in synchronized C3H/10T1/2 cells (*n* = 6) (*F* and *G*) and BMSCs (*n* = 3) (*H* and *I*). Data are expressed as -fold change in gene expression, relative to time 0. *, significantly different from the nadir; *p* < 0.05. Error bars, S.E.

peaking at 4-fold after light removal and decreasing as night progressed. miR-29a and miR-30a expression peaked at ZT17, but the amplitude of their rhythm was more modest in comparison with miR-433 (Fig. 1B).

We also examined the mRNA expression of osteogenic genes previously reported to display circadian rhythmicity *in vivo* (4, 5). Both *Runx2* and *Igf1* mRNAs appeared to peak early in the day, whereas *Hif1α* mRNA displayed a broad peak during each 24-h cycle (Fig. 1, *C* and *D*). In contrast, glucocorticoid receptor (*Nr3c1*) mRNA did not display rhythmic expression in calvaria (Fig. 1*D*).

Development of an in Vitro Model to Study Circadian Rhythm—To better understand the role of miR-433 in circadian rhythm, we used a well established protocol in which the multipotent mouse C3H/10T1/2 cell line and primary mouse bone marrow stromal cells (BMSCs) were synchronized with a pulse of the synthetic glucocorticoid dexamethasone (18, 19). Briefly, C3H/10T1/2 cells and BMSCs were serum-deprived for 24 h and then treated with a 2-h pulse of 100 nM dexamethasone. The dexamethasone was removed (time 0) and replaced with serum-free medium, and RNA was collected for up to 48 h (Fig. 1*E*). The C3H/10T1/2 cells remained synchronized for 48 h, whereas the BMSCs only remained synchronized for ∼30 h. *Bmal1* and *Per2* mRNA expression displayed rhythmic and anti-phasic expression patterns in both C3H/10T1/2 cells and BMSCs, confirming synchronization of the cultures (Fig. 1, *F* and *H*). However, miR-433 did not display rhythmicity in either cell type, suggesting that a systemic factor establishes miR-433 rhythm *in vivo* (Fig. 1, *G* and *I*).

miR-433 Targets the 3′-UTR of Hif1α and Igf1 but Not Per2—To determine whether miR-433 may directly target the circadian clocks, we employed a bioinformatic approach using several online databases (miRanda, TargetScan, and RNAhybrid) to examine complementarity of the miR-433 seed binding region to the 3′-UTR of clock mRNAs (20–22). Of the circadian clock genes, only *Per2* contained a potential miR-433 binding site at position 1829 (Fig. 2*A*). *Runx2*, *Hif1α*, and *Igf1* are rhythmically expressed genes in bone. Whereas *Runx2* was previously confirmed as a miR-433 target (23), *Hif1α* and *Igf1* had yet to be examined. The *Hif1α* 3′-UTR contained two potential miR-433 binding sites at positions 352 and 879; the *Igf1* 3′-UTR contained two potential sites at 4237 and 6113 (Fig. 2*A*). To determine whether *Per2*, *Igf1*, and *Hif1α* were miR-433 targets, target gene 3′-UTRs were cloned downstream of a constitutively expressed luciferase gene in the reporter plasmid pMIR-REPORT. The luciferase constructs containing the target 3′-UTRs were transiently co-transfected into C3H/10T1/2 cells with a non-targeting or miR-433 inhibitor, and luciferase activity was quantified. miR-433 inhibition significantly increased the luciferase activity of *Hif1α* and *Igf1* constructs compared with the non-targeting control, but it did not affect *Per2* 3′-UTR activity (Fig. 2*B*). These data suggest that miR-433 directly targets *Igf1* and *Hif1α* but not *Per2*.

miR-433 Tough Decoy Suppresses miR-433 Activity—To better study the impact of miR-433 on circadian rhythm, we developed a stably transduced C3H/10T1/2 cell line in which the activity of miR-433 could be knocked down in an inducible manner. We used a previously described lentiviral knockdown (pSLIK) system that allows for tight regulation of transgene expression via a doxycycline (Dox)-inducible promoter (24). To achieve knockdown of miR-433 activity, we created a miR-433 tough decoy, in which a *gfp* (green fluorescent protein) reporter carries two miR-
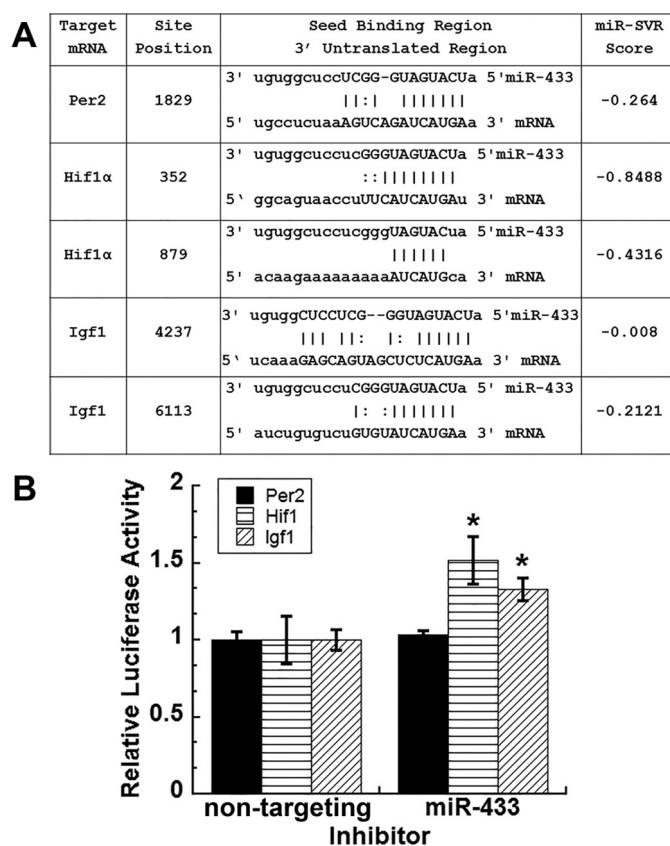
FIGURE 2. **Examination of miR-433 targets.** *A*, potential interaction of miR-433 with *Hif1α*, *Igf1*, and *Per2* 3′-UTRs, as predicted by miRanda (20). *B*, activity of the *Per2*, *Hif1α*, and *Igf1* luciferase-3′-UTR reporter constructs transiently transfected into C3H/10T1/2 cells, along with a miR-433 or non-targeting inhibitor. *, significantly different from non-targeting control; $p < 0.05$ ($n = 12$). *Error bars*, S.E.

433 binding sites in its 3′-UTR (supplemental Fig. S1*A* and Fig. 3*A*) (25). The miR-433 tough decoy contains a secondary structure that enhances resistance to degradation. When transcribed, the miR-433 tough decoy acts as a competitive inhibitor for endogenous miR-433, therefore relieving suppression of its targets. As a control, a C3H/10T1/2 cell line was also established expressing a Dox-inducible non-targeting tough decoy construct.

To confirm doxycycline-inducible expression of the transgene, we quantified GFP mRNA in the non-targeting and miR-433 decoy cells treated for 24 h with increasing doses of Dox. Dox induced *gfp* mRNA in both non-targeting and miR-433 decoy cells in a dose-dependent manner (Fig. 3*B*). To confirm that the decoy inhibited miR-433 actions, we examined luciferase activity of the target 3′-UTR constructs that were previously studied using the transiently transfected miR-433 inhibitor. In these experiments, the miR-433 decoy phenocopied the effects observed with transiently transfected miR-433 inhibitor, with similar increases in luciferase activity with *Igf1* and *Hif1α* 3′-UTR reporter constructs but no change with *Per2* (Fig. 3*C*).

In miR-433 decoy cells, we also examined mRNA levels for a previously defined miR-433 target *Runx2* (23) as well as *Igf1* and *Hif1α*. *Runx2*, *Igf1*, and *Hif1α* mRNA levels were significantly increased after a 24-h treatment with 1000 ng/ml Dox in the miR-433 decoy cells but not in the non-targeting decoy cells

A

pSLIK Inducible System
miR-433 Decoy

+Dox

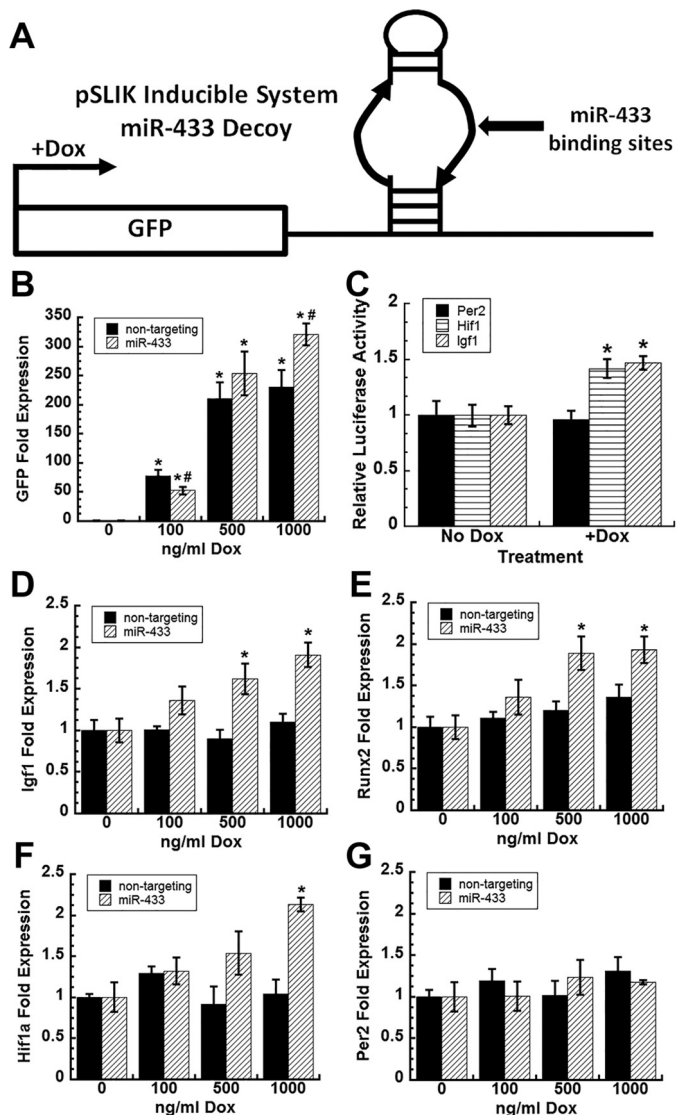GFP

miR-433
binding sites

FIGURE 3. **miR-433 decoy relieves repression of miR-433 target genes *in vitro*.** *A*, C3H/10T1/2 cells were stably transduced with a Dox-inducible construct carrying either a non-targeting or miR-433 decoy in the 3′-UTR of the reporter gene GFP. The location of the miRNA binding site is denoted by the *heavy arrows*. *B*, dose-dependent Dox-mediated induction of non-targeting and miR-433 decoy in C3H/10T1/2 cells. *C*, activity of *Per2*, *Hif1α*, and *Igf1* luciferase-3′ UTR reporter constructs transiently transfected into miR-433 decoy cells cultured in the presence or absence of Dox (*n* = 12). *D–F*, dose-dependent Dox-mediated induction of *Igf1* (*D*), *Runx2* (*E*), and *Hif1α* (*F*) mRNA in miR-433 decoy cells, compared with non-targeting decoy cells (*n* = 4). *G*, *Per2* mRNA was not induced by Dox treatment in either miR-433 or non-targeting decoy cells (*n* = 4). *, significantly different from no Dox control; *p* < 0.05. #, significantly different from non-targeting control; *p* < 0.05. *Error bars*, S.E.

(Fig. 3, *D–F*). In contrast, *Per2* mRNA was unaffected at any dose tested (Fig. 3*G*). Analysis of miR-433 decoy cells at additional time points after Dox treatment also failed to demonstrate significant differences in *Per2* mRNA (data not shown), confirming that *Per2* is not a miR-433 target. Overall, these data demonstrate that the miR-433 decoy inhibits miR-433 activity.

Disruption of miR-433 Activity Impacts the Rhythmicity of the Circadian Clock—Although miR-433 did not display a cell-autonomous rhythm *in vitro*, it is possible that this miRNA could still play a role in maintenance or regulation of rhythm. To examine this *in vitro*, non-targeting and miR-433 decoy cells
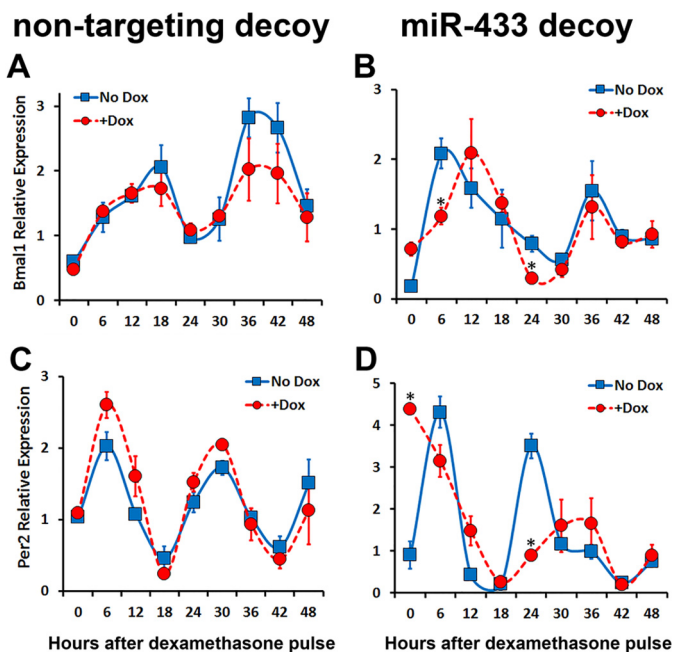

FIGURE 4. **Expression of the miR-433 decoy affects circadian clock mRNA rhythmic expression.** Non-targeting and miR-433 decoy cells were cultured in the absence or presence of 1000 ng/ml doxycycline and then synchronized using a 2-h pulse of 100 nM dexamethasone. mRNA was isolated immediately after the removal of dexamethasone (time 0) and at intervals up to 48 h thereafter. Data are represented as relative expression in non-targeting (*A* and *C*) or miR-433 (*B* and *D*) decoy cells. *A* and *B*, *Bmal1*; *C* and *D*, *Per2*. *, significantly different from the corresponding time point with no Dox treatment; *p* < 0.05 (*n* = 3). *Error bars*, S.E.

were synchronized with a short pulse of dexamethasone, in the presence or absence of Dox. In the synchronized non-targeting decoy cells, both *Bmal1* and *Per2* mRNA displayed two peaks within the 48-h interval. Treatment of the non-targeting decoy cells with Dox did not affect the rhythmicity of either *Bmal1* or *Per2* mRNA (Fig. 4, *A* and *C*). However, in cells expressing the miR-433 decoy, the first peak in *Bmal1* mRNA was shifted from 6 to 12 h (Fig. 4*B*), and the amplitude of the peaks was decreased. For *Per2* mRNA, the effect of miR-433 inhibition was more striking. In miR-433 decoy cells treated with Dox, *Per2* mRNA levels were significantly higher at time 0, and the phase of the *Per2* rhythm was shifted (Fig. 4*D*). Like *Bmal1*, the amplitude of *Per2* mRNA peaks was decreased in the presence of the miR-433 decoy (Fig. 4*D*).

miR-433 Regulates Glucocorticoid Sensitivity—Glucocorticoids play a prominent role in synchronizing the peripheral clocks, in part by activating transcription of *Per* genes (16). Moreover, as circulating glucocorticoids levels fluctuate diurnally, so does the sensitivity of tissues to glucocorticoids. Because miR-433 was previously shown by others to target the glucocorticoid receptor 3′-UTR (15) and because our cell cultures were synchronized using dexamethasone, we hypothesized that miR-433 could help maintain circadian rhythm in cells of the osteoblastic lineage through regulation of glucocorticoid signaling.

Dusp1 and *Per2* are both direct transcriptional targets of the glucocorticoid receptor, and we used their mRNA levels as markers of glucocorticoid signaling (16, 26). In C3H/10T1/2 cells, dexamethasone induced *Dusp1* mRNA at 1–3 h, whereas
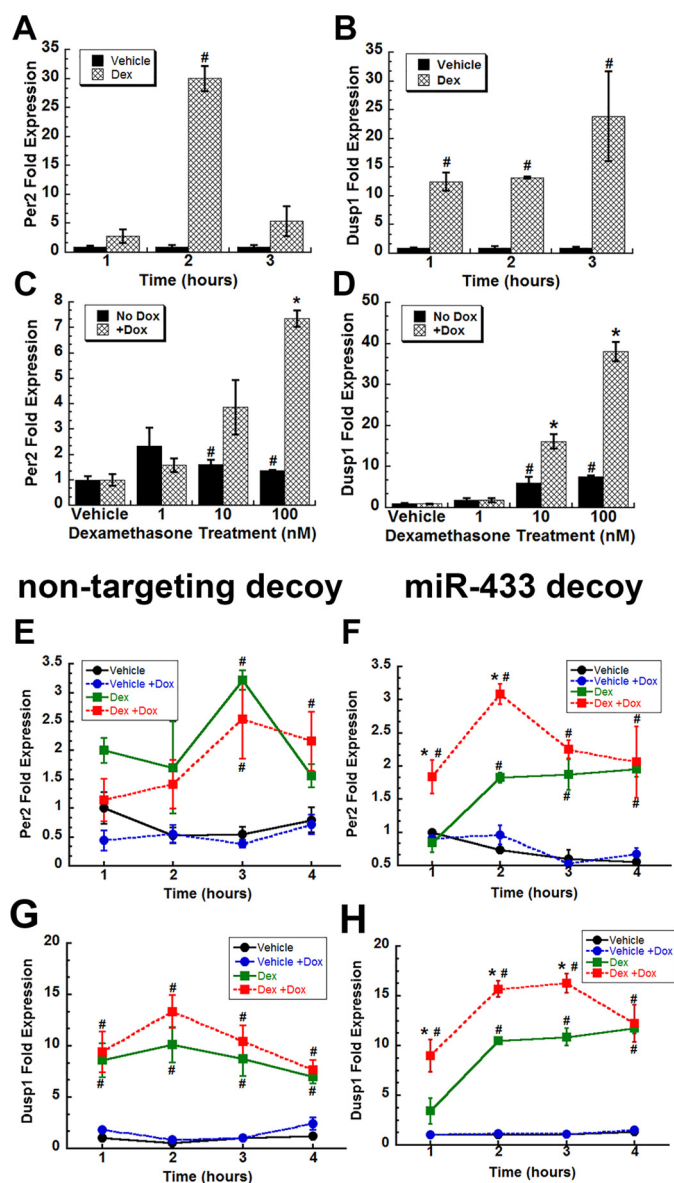
FIGURE 5. **miR-433 dampens sensitivity to glucocorticoid signaling.** *A* and *B*, *Per2* (*A*) and *Dusp1* mRNA (*B*) in serum-deprived C3H/10T1/2 cells treated with vehicle or 100 nM dexamethasone for up to 3 h. *C* and *D*, *Per2* (*C*) and *Dusp1* mRNA levels (*D*) in miR-433 decoy cells that were serum-deprived in the presence or absence of Dox and then treated with increasing doses of dexamethasone for 2 h. *E–H*, *Per2* (*E* and *F*) and *Dusp1* (*G* and *H*) mRNA levels in non-targeting decoy (*E* and *G*) or miR-433 decoy (*F* and *H*) cells that were serum-deprived in the presence or absence of Dox and then treated with vehicle or 100 nM dexamethasone for up to 4 h (*n* = 8). *, significantly different from corresponding no Dox control; *p* < 0.05. #, significantly different from corresponding vehicle-treated control; *p* < 0.05. *Error bars*, S.E.

the increase in *Per2* was more transient, peaking at 2 h (Fig. 5, *A* and *B*). To determine whether miR-433 regulated the sensitivity of cells to glucocorticoids, we examined *Dusp1* and *Per2* mRNA in miR-433 decoy cells treated for 2 h with vehicle or dexamethasone, in the absence or presence of Dox. In the absence of miR-433 decoy, dexamethasone caused a modest increase in *Per2* mRNA, independent of the dose used (Fig. 5*C*). In contrast, expression of the miR-433 decoy augmented the induction of *Per2* mRNA and caused a dose-responsive increase. In the absence of miR-433 decoy, 10 or 100 nM dexamethasone increased *Dusp1* mRNA ~6-fold (Fig. 5*D*). Expression of the

miR-433 decoy further enhanced *Dusp1* mRNA at both 10 and 100 nM dexamethasone (Fig. 5*D*). Because inhibition of miR-433 activity allowed the cells to become responsive to higher levels of glucocorticoids, it is possible that miR-433 functions to limit exposure of cells to excessive glucocorticoid signaling.

We next examined whether miR-433 could regulate the temporal response to glucocorticoid signaling. miR-433 decoy cells were treated with vehicle or 100 nM dexamethasone for up to 4 h, in the absence or presence of Dox, to induce expression of the decoy. In the absence of Dox, dexamethasone increased *Per2* mRNA at 2 h of treatment (Fig. 5*F*). However, when the miR-433 decoy was expressed, the dexamethasone-mediated induction of *Per2* mRNA was accelerated such that *Per2* mRNA was significantly increased after only 1 h of treatment, and its peak expression at 2 h was enhanced. Similarly, in the absence of Dox, dexamethasone modestly increased *Dusp1* mRNA after 1 h of treatment in miR-433 decoy cells (Fig. 5*H*). However, expression of the miR-433 decoy significantly enhanced *Dusp1* mRNA levels at 1–3 h of treatment with dexamethasone. In contrast, in non-targeting decoy cells, the effects of dexamethasone on *Per2* and *Dusp1* mRNAs were similar in the presence or absence of Dox (Fig. 5, *E* and *G*). These data confirm that miR-433 confines glucocorticoid responsiveness.

To determine how miR-433 might regulate sensitivity to glucocorticoid signaling, we first examined the impact of the miR-433 decoy on glucocorticoid receptor mRNA (*Nr3c1*) and protein levels. To mimic the conditions of the circadian synchronization experiments, we performed these studies in cells cultured for 24 h in the presence or absence of Dox and then treated with 100 nM dexamethasone for 2 h. In non-targeting decoy cells, culture in the presence or absence of Dox did not affect mRNA or protein levels of *Nr3c1* (Fig. 6, *A* and *D*). In contrast, miR-433 decoy cells treated with Dox displayed a 3-fold induction of *Nr3c1* mRNA (Fig. 6*A*). However, significant differences in total GR protein levels were not observed at any time point measured (Fig. 6*D*). It is possible that inhibition of miR-433 alters GR mRNA translation efficiency, perhaps by indirectly modifying the complement of miRNAs or RNA-binding proteins interacting with the transcript. GR protein stability could also be affected because GR is subject to ubiquitin-mediated degradation. Overall, these data suggest that an increase in total glucocorticoid receptor levels was not responsible for the increased sensitivity to dexamethasone.

Alternative forms of the mouse glucocorticoid receptor, GRα or GRβ, are generated by alternative splicing (27). It was reported previously that GRα acts as a transcriptional activator of glucocorticoid signaling, whereas GRβ can act as a dominant negative inhibitor of GRα (27–29). Because commercially available antibodies for the mouse glucocorticoid receptor do not discriminate between GRα and GRβ isoforms, we relied on isoform-specific quantitative RT-PCR to determine whether miR-433 inhibition might cause differences in the expression of GRα *versus* GRβ mRNA. miR-433 decoy cells were cultured in the absence or presence of Dox for 24 h and then treated with or without dexamethasone for 2 h. GRα mRNA was increased in miR-433 decoy cells cultured in Dox, and treatment with dexamethasone did not alter GRα mRNA levels (Fig. 6*B*). GRβ mRNA levels were also increased in Dox-treated cells; however,
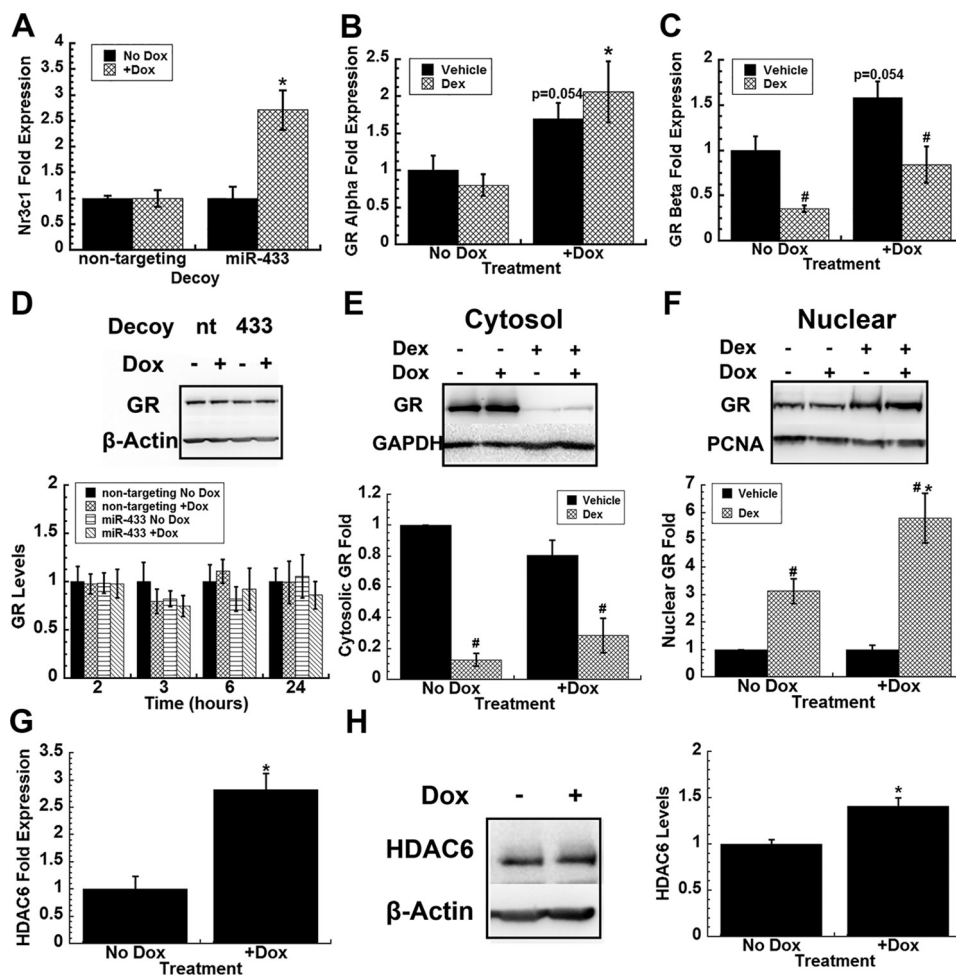
FIGURE 6. **miR-433 regulates glucocorticoid receptor mRNA and subcellular localization.** Non-targeting and miR-433 decoy cells were serum-deprived for 24 h in the presence or absence of Dox and then treated with 100 nM dexamethasone for 2 h. Total glucocorticoid receptor mRNA (*A*) and glucocorticoid receptor mRNA isoforms GRα (*B*) and GRβ (*C*) were quantified (*n* = 8). *D*, miR-433 decoy cells were serum-deprived in the presence or absence of Dox for 24 h and then treated with 100 nM dexamethasone for 2, 3, 6, or 24 h. Total glucocorticoid receptor protein levels were determined by Western blotting (representative blot from a 2-h treatment, *above*) and were quantified (*below*) (*n* = 4). miR-433 decoy cells were serum-deprived for 24 h in the presence or absence of Dox and then treated for 2 h with 100 nM dexamethasone. Glucocorticoid receptor subcellular localization was determined by Western blotting (representative blot, *above*) and were quantified (*below*): cytoplasmic (*E*) and nuclear (*F*) extracts (*n* = 10). miR-433 decoy cells were serum-deprived for 24 h in the absence or presence of Dox, and *Hdac6* mRNA (*G*) and protein (*H*) were quantified (*n* = 7). *, significantly different from corresponding no Dox control; *p* < 0.05. #, significantly different from corresponding vehicle-treated control; *p* < 0.05. *Error bars*, S.E.

dexamethasone decreased GRβ mRNA levels by about 50%, whether the miR-433 decoy was expressed or not (Fig. 6*C*). These data suggest that although dexamethasone affects the mRNA ratio of GRα to GRβ, inhibition of miR-433 activity does not impact this ratio.

Because the miR-433 decoy increased glucocorticoid signaling in the absence of significant increases in GR protein levels or changes in receptor isoform mRNA, we next examined whether miR-433 levels might affect the nuclear *versus* cytosolic localization of the GR. In the absence of ligand, GR is localized primarily in the cytoplasm, in a complex that includes heat shock protein 90, immunophilins, and non-receptor tyrosine kinases (30). Upon ligand binding to the GR, this complex is dissociated, and GR dimers translocate to the nucleus to elicit transcriptional regulation of target genes. We hypothesized that miR-433 inhibition might increase nuclear GR with glucocorticoid stimulation. To test this, miR-433 decoy cells were cultured in the presence or absence of Dox for 24 h and then treated with or without dexamethasone for 2 h. The levels of GR

in nuclear and cytoplasmic compartments were evaluated by Western blotting. In the absence of dexamethasone, the majority of glucocorticoid receptor was found in the cytoplasm, and expression of the miR-433 decoy did not significantly alter its abundance. As expected, when cells were treated with dexamethasone, the abundance of GR in the cytoplasm was dramatically decreased; this decrease was also not significantly affected by expression of the miR-433 decoy (Fig. 6*E*). Examining the nuclear compartment, in the absence of dexamethasone stimulation, GR levels were similar in cells with or without the miR-433 decoy. However, in cells treated with dexamethasone, there was an increase in nuclear GR levels, which was significantly enhanced by expression of the miR-433 decoy (Fig. 6*F*). The enhanced translocation and possibly maintenance of the glucocorticoid receptor to the nucleus upon ligand binding provides a potential mechanism for the enhanced responsiveness of miR-433 decoy cells to dexamethasone.

Heat shock protein 90 (HSP90) plays an important chaperone function for GR in both the cytoplasm and nucleus. Hyper-
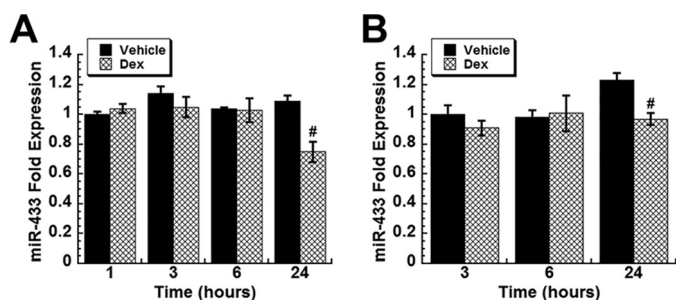
FIGURE 7. **Dexamethasone decreases miR-433 expression.** miR-433 levels in serum-deprived C3H/10T1/2 cells (*A*) or mouse bone marrow stromal cells (*B*) treated with vehicle or 100 nM dexamethasone for up to 24 h. #, significantly different from vehicle control; $p < 0.05$ ($n = 8$). *Error bars*, S.E.

acetylation of HSP90 results in loss of its GR chaperone activity, causing defects in GR ligand binding, nuclear translocation, and transcriptional activation (31, 32). Histone deacetylase 6 (*HDAC6*) can deacetylate HSP90, and in humans, miR-433 has been shown to target *Hdac6* (32). Should the miR-433 decoy increase expression of *Hdac6*, it could represent a potential mechanism for increasing GR nuclear localization. In miR-433 decoy cells cultured in the presence of Dox, *Hdac6* mRNA expression and protein levels were significantly increased (Fig. 6, *G* and *H*), indicating that miR-433 targets *Hdac6* in mice as well as humans. miR-433 effects on *Hdac6* could contribute to its regulation of glucocorticoid sensitivity.

Glucocorticoids Down-regulate miR-433—Because microRNAs often participate in feedback loops, we determined whether glucocorticoids might regulate the expression of miR-433. In serum-deprived C3H/10T1/2 cells treated with 100 nM dexamethasone for up to 24 h, we found a modest (20–25%) but significant reduction of miR-433 only at the 24 h time point (Fig. 7*A*). Serum-deprived confluent cultures of primary BMSCs displayed a similar decrease in miR-433 expression with dexamethasone treatment (Fig. 7*B*). This delay in response suggests that dexamethasone may indirectly regulate miR-433 expression, or it could reflect the generally high stability of many miRNAs.

miR-433 Regulates Circadian Clocks and Osteoblastic Genes in Vivo—Our *in vitro* studies indicated that miR-433 activity dampens glucocorticoid signaling and is important for maintaining rhythmic gene expression in osteoblastic cells. To determine whether miR-433 plays a similar role in the regulation of the circadian clocks *in vivo*, we developed a transgenic mouse model in which the miR-433 decoy, contained within the 3′-UTR of the red fluorescent reporter gene tdTomato, was expressed under the control of a 3.6-kb fragment of the rat *Col1a1* promoter (miR-433 decoy[Col1a1] mice) (Fig. 8 and supplemental Fig. S1C). Previous studies document that transgenes under the control of this promoter are expressed most abundantly in osteoblastic cells, with lesser expression in other type I collagen-containing tissues (33, 34). Fluorescence microscopy of calvarial sections from miR-433 decoy[Col1a1] mice demonstrated that signal for tdTomato was localized to osteocytes embedded in the bone matrix and cells on the periosteal and endosteal surfaces, where new bone is formed (Fig. 8*A*).
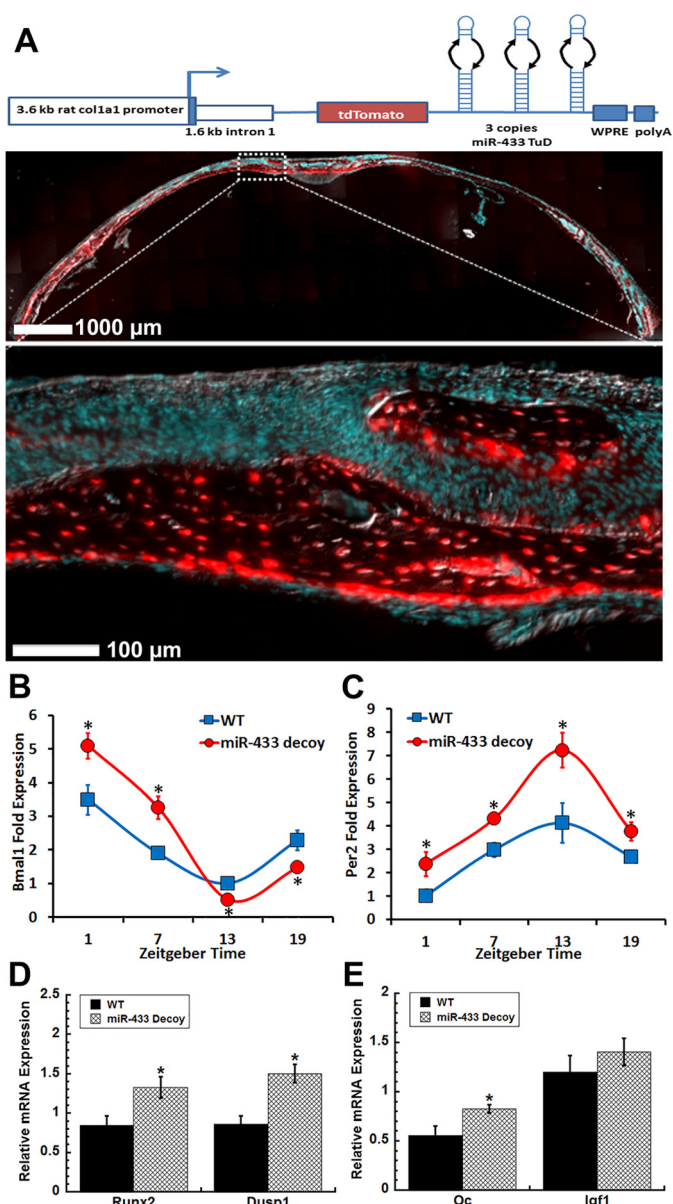

FIGURE 8. **miR-433 regulation of circadian clocks and osteoblast genes *in vivo*.** Calvaria were isolated from male transgenic mice expressing the miR-433 decoy under the control of a *Col1a1* promoter (miR-433 decoy[Col1a1] mice) and wild type littermate controls. *A*, schematic of Col3.6/1.6_tdTomato_miR-433 decoy transgene cassette. A 3.6-kb fragment of the rat *Col1a1* gene plus the first intron drive expression of the reporter gene tdTomato and a 3′-UTR containing three copies of a miR-433 tough decoy (miR-433 binding sites are denoted by *black arrows*), a woodchuck hepatitis virus posttranscriptional regulatory element (*WPRE*), and bovine growth hormone polyadenylation signal (*polyA*). Shown is an example of td Tomato transgene and DAPI fluorescence in a calvarium from a 4-week-old male miR-433 decoy[Col1a1] mouse at ZT13. *B* and *C*, mRNA levels from calvaria of 8-week-old mice for *Bmal1* (*B*) and *Per2* (*C*) at ZT1, ZT7, ZT13, and ZT19. *Runx2* and *Dusp1* (*D*) and osteocalcin (*Oc*) and *Igf1* (*E*) mRNA were quantified in calvaria at ZT13. Shown are pooled data from two miR-433 decoy[Col1a1] lines having a similar level of transgene expression. $n = 7$ for WT; $n = 8$ for miR-433 decoy[Col1a1]. *, significantly different WT littermates; $p < 0.05$. *Error bars*, S.E.

To determine the impact of miR-433 on circadian rhythm, RNA was isolated from calvaria of 8-week-old male miR-433 decoy[Col1a1] mice and matched litter mate controls euthanized every 6 h over an 18-h period. *Bmal1* and *Per2* mRNA expression showed rhythmic and anti-phasic expression in both wild type and miR-433 decoy[Col1a1] mice (Fig. 8, *B* and *C*). However,

the amplitude of *Bmal1* mRNA rhythm in miR-433 decoy[Col1a1] mice was significantly increased compared with littermate controls (Fig. 8*B*). The amplitude of *Per2* mRNA rhythm was also significantly increased in miR-433 decoy[Col1a1] mice (Fig. 8*C*). Thus, miR-433 dampens the rhythm of circadian clock genes *in vivo*, supporting its role in the regulation of circadian rhythm.

miR-433 can directly target *Runx2* and *Igf1*, suggesting that it may negatively regulate osteoblastogenesis (23). Indeed, calvaria from miR-433 decoy[Col1a1] mice had 1.5-fold higher levels of *Runx2* mRNA as well as elevated mRNA for the RUNX2 target gene, osteocalcin (Fig. 8, *D* and *E*). Expression of the glucocorticoid-responsive gene *Dusp1* was also increased ~2-fold in bone from miR-433 decoy[Col1a1] mice (Fig. 8*D*). In contrast, *Igf1* mRNA was similar in wild type and miR-433 decoy[Col1a1] mice (Fig. 8*E*). Overall, inhibition of miR-433 activity increased the expression of glucocorticoid-responsive genes and increased expression of a subset of osteoblast marker genes *in vivo*, supporting *in vitro* observations.

Discussion

The circadian clocks are crucial regulators of organismal physiology and behavior, operating through a series of positive and negative feedback loops, the regulation of which includes microRNAs. In this study, we demonstrate that miR-433 displays a robust rhythmic expression in the calvaria and that miR-433 is important in maintaining the rhythmic expression of the circadian clocks *in vitro* and *in vivo*. miR-433 serves to limit the responsiveness of mesenchymal cells to glucocorticoids, which could contribute to its regulation of circadian rhythm. In addition, we identified two novel targets of miR-433, *Igf1* and *Hif1α*, both of which display rhythmicity *in vivo* and play an important role in osteogenesis. Altogether, we showed that miR-433 can modify responsiveness of cells to glucocorticoids, providing a potential mechanism contributing to its ability to regulate rhythmic gene expression in bone and possibly other tissues.

Although microRNAs were shown to be important regulators of circadian rhythm in non-skeletal tissues (11, 12, 14), to our knowledge, this is the first study examining the role of miRNAs in circadian rhythm in bone. In our study, miR-433 displayed a sizeable rhythmicity in the calvaria, and its rhythm had a larger amplitude compared with miR-29a and miR-30a, two microRNAs previously shown to display significant rhythmicity in the liver (10). It is likely that other miRNAs display circadian rhythm in the calvaria, and this remains to be examined.

miRNAs can regulate circadian rhythm through direct targeting of the circadian clocks, by regulation of entrainment, or by reducing target mRNAs' oscillation amplitude or frequency (35). Several miRNAs have been found to impact circadian rhythms in the liver, with miR-122 being the most studied. The miR-122 locus is under the direct regulation of REV-ERBα, an important circadian protein that functions by recruiting histone deacetylases (HDACs), repressing gene expression (36). Systemic administration of miR-122 antisense oligonucleotides caused substantial alterations in amplitude, magnitude, and phase of several rhythmic mRNAs in the liver, with corresponding changes in expression of genes involved in cholesterol and lipid metabolism (36). Whereas previous studies examined the direct regulation of miRNAs on the circadian clocks, our study

suggests that miR-433 regulation of glucocorticoid signaling in peripheral tissues could impact the rhythmic expression of the circadian clocks *in vivo* (*i.e.* synchrony).

Glucocorticoids, among other hormones, are important entrainment signals that synchronize circadian rhythms in the kidney, liver, heart, and other tissues (37). High levels of glucocorticoids can disrupt circadian rhythm (38). In humans, serum levels of glucocorticoids cycle, with their peak in the early morning, just before waking, and their lowest levels in the evening (39). The circadian clocks can be directly regulated by glucocorticoid signaling, as the glucocorticoid receptor transcriptionally activates expression of *Per1* through a glucocorticoid response element (GRE) in its promoter and *Per2* through a GRE in the first intron (16, 40, 41). Indeed, oscillating levels of circulating glucocorticoids correspond to Per1 levels in peripheral tissues (42).

Glucocorticoid receptor-induced transcriptional activity can also be directly suppressed by CLOCK, which assists with acetylating the GR hinge domain (17, 43). This acetylation attenuates the binding of the GR to GREs, limiting its actions. In peripheral tissues, the BMAL1/CLOCK-mediated counter-regulation of glucocorticoid signaling provides a mechanism to prevent overexposure of target tissues to glucocorticoids at times when serum levels of glucocorticoid are at their peak (1). Similarly, we demonstrate that miR-433 activity blunts glucocorticoid signaling. In mice, miR-433 levels peak just after dark (Fig. 1), and serum glucocorticoids peak just before dark (44). In calvaria of miR-433 decoy[Col1a1] mice, we observed increased mRNA for the glucocorticoid receptor target genes *Per2* and *Dusp1* (Fig. 8), further supporting the concept that miR-433 serves as an additional mechanism to limit exposure of osteoblastic cells to glucocorticoids *in vivo*.

In humans, miR-433 has been shown to target the *HDAC6* 3′-UTR (32), and we showed that inhibition of miR-433 enhanced *Hdac6* mRNA and protein. miR-433 could regulate the acetylation status of HDAC6 targets, including the glucocorticoid receptor or its chaperone HSP90, as well as many other targets. As discussed previously, hyperacetylation of HSP90 compromises its GR chaperone activity, causing defects in GR ligand binding, nuclear translocation, and transcriptional activation (31, 32). Our results indicate that miR-433 can regulate the sensitivity of cells to glucocorticoids through decreasing translocation of the GR to the nucleus. It is possible that miR-433 controls HSP90 acetylation and chaperone function by targeting *Hdac6*, fine tuning glucocorticoid responsiveness.

The role of glucocorticoid signaling in bone is complex. Normal, endogenous glucocorticoids are critical for skeletal health (for a review, see Ref. 45). Glucocorticoids can enhance the expression of osteoblast differentiation markers, such as alkaline phosphatase, osteocalcin, and bone sialoprotein, *in vitro* (for a review, see Ref. 46). In contrast, excessive exposure of the skeleton to glucocorticoids leads to the development of osteoporosis, which is frequently seen in patients treated long term with glucocorticoids for autoimmune disorders, inflammatory disease, or malignancy. Glucocorticoid excess causes bone loss due to decreased osteoblast activity, reduced osteoblast number, increased osteocyte apoptosis, and disruption of extracellular matrix production (for a review, see Ref. 47). In our *in vivo*

model, calvaria from mice expressing the miR-433 decoy in osteoblastic cells had increased mRNA for *Runx2* and its downstream target, osteocalcin. This was not unexpected, because miR-433 was previously shown to target *Runx2* (23). That *Igf1* was not similarly increased suggests that other mechanisms, transcriptional or post-transcriptional, predominate in the regulation of this gene *in vivo*. We are in the process of fully characterizing the skeletal phenotype of miR-433 decoy[Col1a1] mice to better understand the function of miR-433 in bone.

We identified two new miR-433 targets, *Hif1α* and *Igf1*, which have been shown to be to be important factors in bone formation and homeostasis (48 –51). IGF1 enhances osteoblast differentiation and induces osteoblast proliferation (50). HIF1α is important in coupling angiogenic and osteogenic activity, to promote bone formation (49, 51). In calvaria, miR-433 levels are highest when mRNA levels of its targets, *Runx2* and *Igf1*, are the lowest. In contrast, the peak of miR-433 coincides with a broad peak in *Hif1α* mRNA. It is possible that miR-433 serves to fine tune expression of this regulator.

Transcription of the miR-433 locus has been shown to be induced by orphan receptor estrogen-related receptor γ (ERRγ), a negative regulator of osteogenesis, whereas its transcription can be repressed by small heterodimer partner (SHP), which promotes osteoblast differentiation (23, 52, 53). Although estrogen-related receptors have been linked to energy homeostasis and can display circadian regulation, it is not known whether these mechanisms are active in calvaria (54, 55). Disruption of normal circadian rhythm, resulting in changes of clock amplitude, period length, or frequency, lead to alterations in chromatin modification, gene regulation, cellular metabolism, and immune responses (56). Consequently, chronic desynchrony is associated with the development and progression of cardiovascular disease, cancer, mental illnesses, and severe metabolic disorders (for a review, see Ref. 57).

Overall, we found that miR-433 displays rhythmicity in calvaria, regulates cell sensitivity to glucocorticoids, and helps maintain rhythmic gene expression. Because miR-433 levels in bone peak when circulating glucocorticoid levels are high, it probably plays a role in balancing the glucocorticoid response. We speculate that miR-433 can modify the responsiveness of peripheral tissues to variations in circulating glucocorticoids and alter bone metabolism. miR-433 also targets *Hdac6*, providing a mechanism for modulating the acetylation status of multiple HDAC6 targets. These findings provide an added dimension to our understanding of the mechanisms regulating glucocorticoid responsiveness, circadian rhythm, and their potential impact on the skeleton and possibly other tissues.

Experimental Procedures

Mice—C57BL/6 male mice were kept under a 12-h light/dark cycle and provided with food and water *ad libitum*. Eight-week-old male mice were euthanized every 4 h, and calvaria were collected.

We created mice expressing a transgene in which a 3.6-kb fragment of the rat *Col1A1* promoter, plus 1.6 kb of the first intron drive expression of the tdTomato reporter gene carrying a miR-433 tough decoy in its 3′-UTR (custom synthesis, GenScript, Piscataway, NJ) (Fig. 8*A* and supplemental Fig. S1*C*) (25, 33). Mice were generated in a C57BL/6 background by pronuclear injection of the transgene cassette at the UConn Health Gene Targeting and Transgenic Facility. The miR-433 decoy serves as a competitive inhibitor of miR-433 activity, relieving the suppression of endogenous miR-433 targets. The sequence of the miR-433 tough decoy is provided in supplemental Fig. S1*C*. Eight-week-old male transgenic mice and wild type littermates were euthanized every 6 h, and calvaria were collected.

All animal protocols were reviewed and approved by the UConn Health institutional animal care and use committee.

Cell Culture and Synchronization—C3H/10T1/2, clone 8, a multipotent mouse mesenchymal cell line, was obtained from the American Type Culture Collection (ATCC, CCL-226) and cultured in DMEM (Gibco) supplemented with 10% heat-inactivated FBS (Lonza, Basel, Switzerland). Primary BMSCs were flushed from the long bones of 6 – 8-week-old male C57BL/6 mice and maintained in DMEM supplemented with 10% FBS. Cells were synchronized by 24 h of serum deprivation, followed by treatment for 2 h with 100 nM dexamethasone (Sigma-Aldrich). The dexamethasone was then replaced with serum-free medium for the remainder of the experiment (19). Amplitude was determined by calculating the difference between a peak and the mean value of the wave.

Quantitative Real-time PCR—Total RNA from calvaria samples was extracted using the miRNeasy minikit (Qiagen, Valencia, CA). Calvaria were homogenized in Qiazol. RNA was isolated from cell cultures using TRIzol reagent (Life Technologies, Inc.). RNA samples were DNased using RQ1 DNase (Promega, Madison, WI). DNased RNA was reverse-transcribed using Moloney murine leukemia virus-reverse transcriptase (Invitrogen). Gene expression was quantified by quantitative PCR with iQ SYBR Green Supermix (Bio-Rad) and normalized to 18S rRNA. Primer sets are shown in supplemental Table S1. MicroRNA expression levels were analyzed using the TaqMan microRNA assay (Life Technologies). RNA was reverse transcribed with gene-specific primers to generate cDNA. MicroRNA expression was detected by quantitative PCR and normalized to snoRNA 202. Each sample was assayed in duplicate.

Luciferase Assay—Gene-specific PCR primers were used to amplify from genomic DNA template the 3′-UTR for *Igf1* (mouse, bp 1– 6217), *HIF1α* (human, bp 2612–3906), and *PER2* (human, bp 866 –2041). These fragments were subcloned downstream of a cytomegalovirus promoter-driven luciferase reporter (pMIR-REPORT vector, Ambion, Carlsbad, CA). Constructs were verified by sequencing.

C3H/10T11/2 cells were plated at 25,000 cells/cm^2. BioT transfection reagent (1.5 μl per 1 μg of DNA; Bioland Scientific, Paramount, CA) was used to co-transfect luciferase constructs containing the 3′-UTR of target mRNA, a constitutively active β-galactosidase construct (control for transfection efficiency), and miRNA hairpin inhibitors (Dharmacon/Thermo Fisher Scientific, Waltham, MA). 80 nM miR-433 or negative control (non-targeting) miRNA inhibitors were used. Cell lysates were analyzed for luciferase activity using the Luciferase assay system (Promega) and normalized to β-galactosidase using Galacton® (Life Technologies). More than one preparation of each DNA construct was tested.

Establishment of a Stable Inducible miR-433 Knockdown Model—To achieve knockdown of miR-433 activity, C3H/10T11/2 cells were transduced using lentiviral constructs containing a miR-433 tough decoy (custom synthesis, GenScript) driven by a Dox-inducible promoter. The miR-433 decoy contains complementary sites that will bind endogenous miR-433. The miR-433 decoy was subcloned into the single lentivector for inducible knockdown (pSLIK) system and confirmed by sequencing (24) (Addgene, Cambridge, MA). Doxycycline treatment stimulates the decoy. As a control, we developed a non-targeting tough decoy containing *Caenorhabditis elegans* miR-67 binding sites (custom synthesis, GenScript), which is not predicted to interact with mammalian miRNAs. Pools of cells stably transduced with the pSLIK-miR-433 decoy or non-targeting decoy were selected for hygromycin resistance. The sequence for the miR-433 and non-targeting decoy may be found in supplemental Fig. S1, *A and B*.

Western Blotting—C3H/10T1/2 cells were plated at 200,000 cells/cm^2 and treated with doxycyline for 24 h in serum-free medium to induce expression of the decoy. Cells were lysed with radioimmune precipitation buffer containing Halt^{TM} protease inhibitors (Thermo Fisher Scientific). A BCA assay (Thermo Fisher Scientific) was performed to quantify protein, and 20 μg of protein was subjected to electrophoresis on a 10% SDS-polyacrylamide gel. Proteins were transferred to a PVDF membrane (Millipore, Billerica, MA). Rabbit anti-mouse glucocorticoid receptor primary antibody (1:1000; Cell Signaling (Danvers, MA), D6H2L), rabbit anti-HDAC6 antibody (1:1000; Cell Signaling, D21B10), rabbit anti-β-actin antibody (1:2000; Cell Signaling, 13E5), and goat anti-rabbit horseradish peroxidase-conjugated antibody (1:10,000; Sigma-Aldrich, A0545) were used.

To analyze nuclear *versus* cytosolic localization of the glucocorticoid receptor, C3H/10T1/2 cells were serum-deprived for 24 h, in the presence or absence of doxycycline, and then treated with or without 100 nM dexamethasone for 2 h. Cells were trypsinized and pelleted. Pellets were suspended in a cytosolic extraction buffer (10 mM Hepes, 60 mM KCl, 1 mM EDTA, 0.075% Igepal 40, 1 mM DTT, and 1 mM PMSF). The lysate was pelleted, and the supernatant was collected as the cytosolic fraction. Pellets were resuspended in nuclear extraction buffer (20 mM Tris-Cl, 420 mM NaCl, 1.5 mM MgCl$_2$, 0.2 mM EDTA, 1 mM PMSF, and 25% glycerol) and then pelleted; the supernatant was collected as the nuclear fraction. Half of each lysate was subjected to electrophoresis on a 10% SDS-polyacrylamide gel and transferred to PVDF membrane, and the same antibody dilutions as noted above were used for the glucocorticoid receptor and β-actin. For the nuclear fraction, rabbit anti-mouse proliferating cell nuclear antigen was used to control for loading (1:2000; Cell Signaling, 13110P). Chemiluminescent signal was achieved using SuperSignal West Pico Kit (Thermo Fisher Scientific) and captured using the Bio-Rad ChemiDoc XRS+ imaging system. Densitometry of protein bands was performed using ImageJ analysis (58). Levels of the glucocorticoid receptor were normalized to either β-actin or proliferating cell nuclear antigen.

Cryohistology and Microscopy Imaging—Calvaria from 4-week-old male mice were fixed (4% paraformaldehyde),

decalcified (14% EDTA-acid, 0.9% ammonium hydroxide), and washed in a 30% sucrose PBS solution at 4 °C. Samples were embedded in O.C.T. compound (VWR, Radnor, PA). 7-μm sections were collected with a Cryofilm type II tape transfer system (Section Lab Co. Ltd., Hiroshima, Japan). Sections were mounted for imaging (50% glycerol buffered with PBS containing 0.2 mg/ml DAPI; Thermo Scientific Fisher), imaged with a Zeiss Observer Z.1 microscope, and captured using an Axiocam MRc digital camera and Axiovision software (Zeiss).

Statistics—All data are represented as mean ± S.E. Statistical significance was determined using two-tailed analysis of variance with Bonferroni post hoc test or Student's *t* test as appropriate (KaleidaGraph, Synergy Software, Reading, PA).

References

1. Gimble, J. M., Floyd, Z. E., and Bunnell, B. A. (2009) The 4th dimension and adult stem cells: can timing be everything? *J. Cell Biochem.* **107,** 569–578
2. Reppert, S. M., and Weaver, D. R. (2002) Coordination of circadian timing in mammals. *Nature* **418,** 935–941
3. Eckel-Mahan, K., and Sassone-Corsi, P. (2013) Metabolism and the circadian clock converge. *Physiol. Rev.* **93,** 107–135
4. Witt-Enderby, P. A., Slater, J. P., Johnson, N. A., Bondi, C. D., Dodda, B. R., Kotlarczyk, M. P., Clafshenkel, W. P., Sethi, S., Higginbotham, S., Rutkowski, J. L., Gallagher, K. M., and Davis, V. L. (2012) Effects on bone by the light/dark cycle and chronic treatment with melatonin and/or hormone replacement therapy in intact female mice. *J. Pineal Res.* **53,** 374–384
5. Kawai, M., Delany, A. M., Green, C. B., Adamo, M. L., and Rosen, C. J. (2010) Nocturnin suppresses igf1 expression in bone by targeting the 3′ untranslated region of igf1 mRNA. *Endocrinology* **151,** 4861–4870
6. Zvonic, S., Ptitsyn, A. A., Kilroy, G., Wu, X., Conrad, S. A., Scott, L. K., Guilak, F., Pelled, G., Gazit, D., and Gimble, J. M. (2007) Circadian oscillation of gene expression in murine calvarial bone. *J. Bone Miner. Res.* **22,** 357–365
7. Hassager, C., Risteli, J., Risteli, L., Jensen, S. B., and Christiansen, C. (1992) Diurnal variation in serum markers of type I collagen synthesis and degradation in healthy premenopausal women. *J. Bone Miner. Res.* **7,** 1307–1311
8. Pietschmann, P., Resch, H., Woloszczuk, W., and Willvonseder, R. (1990) A circadian rhythm of serum osteocalcin levels in postmenopausal osteoporosis. *Eur J. Clin. Invest.* **20,** 310–312
9. Heshmati, H. M., Riggs, B. L., Burritt, M. F., McAlister, C. A., Wollan, P. C., and Khosla, S. (1998) Effects of the circadian variation in serum cortisol on markers of bone turnover and calcium homeostasis in normal postmenopausal women. *J. Clin. Endocrinol. Metab.* **83,** 751–756
10. Vollmers, C., Schmitz, R. J., Nathanson, J., Yeo, G., Ecker, J. R., and Panda, S. (2012) Circadian oscillations of protein-coding and regulatory RNAs in a highly dynamic mammalian liver epigenome. *Cell Metab.* **16,** 833–845
11. Xu, S., Witmer, P. D., Lumayag, S., Kovacs, B., and Valle, D. (2007) MicroRNA (miRNA) transcriptome of mouse retina and identification of a sensory organ-specific miRNA cluster. *J. Biol. Chem.* **282,** 25053–25066

12. Na, Y. J., Sung, J. H., Lee, S. C., Lee, Y. J., Choi, Y. J., Park, W. Y., Shin, H. S., and Kim, J. H. (2009) Comprehensive analysis of microRNA-mRNA co-expression in circadian rhythm. *Exp. Mol. Med.* **41,** 638–647

13. Kojima, S., Gatfield, D., Esau, C. C., and Green, C. B. (2010) MicroRNA-122 modulates the rhythmic expression profile of the circadian deadenylase Nocturnin in mouse liver. *PLoS One* **5,** e11264

14. Cheng, H. Y., Papp, J. W., Varlamova, O., Dziema, H., Russell, B., Curfman, J. P., Nakazawa, T., Shimizu, K., Okamura, H., Impey, S., and Obrietan, K. (2007) microRNA modulation of circadian-clock period and entrainment. *Neuron* **54,** 813–829

15. Riester, A., Issler, O., Spyroglou, A., Rodrig, S. H., Chen, A., and Beuschlein, F. (2012) ACTH-dependent regulation of microRNA as endogenous modulators of glucocorticoid receptor expression in the adrenal gland. *Endocrinology* **153,** 212–222

16. Reddy, T. E., Gertz, J., Crawford, G. E., Garabedian, M. J., and Myers, R. M. (2012) The hypersensitive glucocorticoid response specifically regulates period 1 and expression of circadian genes. *Mol. Cell Biol.* **32,** 3756–3767

17. Nicolaides, N. C., Charmandari, E., Chrousos, G. P., and Kino, T. (2014) Recent advances in the molecular mechanisms determining tissue sensitivity to glucocorticoids: novel mutations, circadian rhythm and ligand-induced repression of the human glucocorticoid receptor. *BMC Endocr. Disord.* **14,** 71

18. Wu, X., Yu, G., Parks, H., Hebert, T., Goh, B. C., Dietrich, M. A., Pelled, G., Izadpanah, R., Gazit, D., Bunnell, B. A., and Gimble, J. M. (2008) Circadian mechanisms in murine and human bone marrow mesenchymal stem cells following dexamethasone exposure. *Bone* **42,** 861–870

19. Merrill, G. F. (1998) Cell synchronization. *Methods Cell Biol.* **57,** 229–249

20. Betel, D., Koppal, A., Agius, P., Sander, C., and Leslie, C. (2010) Comprehensive modeling of microRNA targets predicts functional non-conserved and non-canonical sites. *Genome Biol.* **11,** R90

21. Lewis, B. P., Burge, C. B., and Bartel, D. P. (2005) Conserved seed pairing, often flanked by adenosines, indicates that thousands of human genes are microRNA targets. *Cell* **120,** 15–20

22. Rehmsmeier, M., Steffen, P., Hochsmann, M., and Giegerich, R. (2004) Fast and effective prediction of microRNA/target duplexes. *RNA* **10,** 1507–1517

23. Kim, E. J., Kang, I. H., Lee, J. W., Jang, W. G., and Koh, J. T. (2013) MiR-433 mediates ERRγ-suppressed osteoblast differentiation via direct targeting to Runx2 mRNA in C3H10T1/2 cells. *Life Sci.* **92,** 562–568

24. Shin, K. J., Wall, E. A., Zavzavadjian, J. R., Santat, L. A., Liu, J., Hwang, J. I., Rebres, R., Roach, T., Seaman, W., Simon, M. I., and Fraser, I. D. (2006) A single lentiviral vector platform for microRNA-based conditional RNA interference and coordinated transgene expression. *Proc. Natl. Acad. Sci. U.S.A.* **103,** 13759–13764

25. Haraguchi, T., Ozaki, Y., and Iba, H. (2009) Vectors expressing efficient RNA decoys achieve the long-term suppression of specific microRNA activity in mammalian cells. *Nucleic Acids Res.* **37,** e43

26. Shipp, L. E., Lee, J. V., Yu, C. Y., Pufall, M., Zhang, P., Scott, D. K., and Wang, J. C. (2010) Transcriptional regulation of human dual specificity protein phosphatase 1 (DUSP1) gene by glucocorticoids. *PLoS One* **5,** e13754

27. Hinds, T. D., Jr., Ramakrishnan, S., Cash, H. A., Stechschulte, L. A., Heinrich, G., Najjar, S. M., and Sanchez, E. R. (2010) Discovery of glucocorticoid receptor-β in mice with a role in metabolism. *Mol. Endocrinol.* **24,** 1715–1727

28. Bamberger, C. M., Bamberger, A. M., de Castro, M., and Chrousos, G. P. (1995) Glucocorticoid receptor β, a potential endogenous inhibitor of glucocorticoid action in humans. *J. Clin. Invest.* **95,** 2435–2441

29. Bamberger, C. M., Schulte, H. M., and Chrousos, G. P. (1996) Molecular determinants of glucocorticoid receptor function and tissue sensitivity to glucocorticoids. *Endocr. Rev.* **17,** 245–261

30. Cain, D. W., and Cidlowski, J. A. (2015) Specificity and sensitivity of glucocorticoid signaling in health and disease. *Best Pract. Res. Clin. Endocrinol. Metab.* **29,** 545–556

31. Kovacs, J. J., Murphy, P. J., Gaillard, S., Zhao, X., Wu, J. T., Nicchitta, C. V., Yoshida, M., Toft, D. O., Pratt, W. B., and Yao, T. P. (2005) HDAC6 regulates Hsp90 acetylation and chaperone-dependent activation of glucocorticoid receptor. *Mol. Cell* **18,** 601–607

32. Simon, D., Laloo, B., Barillot, M., Barnetche, T., Blanchard, C., Rooryck, C., Marche, M., Burgelin, I., Coupry, I., Chassaing, N., Gilbert-Dussardier, B., Lacombe, D., Grosset, C., and Arveiler, B. (2010) A mutation in the 3′-UTR of the HDAC6 gene abolishing the post-transcriptional regulation mediated by hsa-miR-433 is linked to a new form of dominant X-linked chondrodysplasia. *Hum. Mol. Genet.* **19,** 2015–2027

33. Kalajzic, I., Kalajzic, Z., Kaliterna, M., Gronowicz, G., Clark, S. H., Lichtler, A. C., and Rowe, D. (2002) Use of type I collagen green fluorescent protein transgenes to identify subpopulations of cells at different stages of the osteoblast lineage. *J. Bone Miner. Res.* **17,** 15–25

34. Kalajzic, Z., Liu, P., Kalajzic, I., Du, Z., Braut, A., Mina, M., Canalis, E., and Rowe, D. W. (2002) Directing the expression of a green fluorescent protein transgene in differentiated osteoblasts: comparison between rat type I collagen and rat osteocalcin promoters. *Bone* **31,** 654–660

35. Nandi, A., Vaz, C., Bhattacharya, A., and Ramaswamy, R. (2009) miRNA-regulated dynamics in circadian oscillator models. *BMC Syst. Biol.* **3,** 45

36. Gatfield, D., Le Martelot, G., Vejnar, C. E., Gerlach, D., Schaad, O., Fleury-Olela, F., Ruskeepää, A. L., Oresic, M., Esau, C. C., Zdobnov, E. M., and Schibler, U. (2009) Integration of microRNA miR-122 in hepatic circadian gene expression. *Genes Dev.* **23,** 1313–1326

37. Balsalobre, A., Brown, S. A., Marcacci, L., Tronche, F., Kellendonk, C., Reichardt, H. M., Schütz, G., and Schibler, U. (2000) Resetting of circadian time in peripheral tissues by glucocorticoid signaling. *Science* **289,** 2344–2347

38. Chung, S., Son, G. H., and Kim, K. (2011) Circadian rhythm of adrenal glucocorticoid: its regulation and clinical implications. *Biochim. Biophys. Acta* **1812,** 581–591

39. Nader, N., Chrousos, G. P., and Kino, T. (2010) Interactions of the circadian CLOCK system and the HPA axis. *Trends Endocrinol. Metab.* **21,** 277–286

40. So, A. Y., Bernal, T. U., Pillsbury, M. L., Yamamoto, K. R., and Feldman, B. J. (2009) Glucocorticoid regulation of the circadian clock modulates glucose homeostasis. *Proc. Natl. Acad. Sci. U.S.A.* **106,** 17582–17587

41. Segall, L. A., and Amir, S. (2010) Glucocorticoid regulation of clock gene expression in the mammalian limbic forebrain. *J. Mol. Neurosci.* **42,** 168–175

42. Son, G. H., Chung, S., Choe, H. K., Kim, H. D., Baik, S. M., Lee, H., Lee, H. W., Choi, S., Sun, W., Kim, H., Cho, S., Lee, K. H., and Kim, K. (2008) Adrenal peripheral clock controls the autonomous circadian rhythm of glucocorticoid by causing rhythmic steroid production. *Proc. Natl. Acad. Sci. U.S.A.* **105,** 20970–20975

43. Nader, N., Chrousos, G. P., and Kino, T. (2009) Circadian rhythm transcription factor CLOCK regulates the transcriptional activity of the glucocorticoid receptor by acetylating its hinge region lysine cluster: potential physiological implications. *FASEB J.* **23,** 1572–1583

44. Oishi, K., Ohkura, N., Kadota, K., Kasamatsu, M., Shibusawa, K., Matsuda, J., Machida, K., Horie, S., and Ishida, N. (2006) Clock mutation affects circadian regulation of circulating blood cells. *J. Circadian Rhythms* **4,** 13

45. Delany, A. M., Dong, Y., and Canalis, E. (1994) Mechanisms of glucocorticoid action in bone cells. *J. Cell Biochem.* **56,** 295–302

46. Moutsatsou, P., Kassi, E., and Papavassiliou, A. G. (2012) Glucocorticoid receptor signaling in bone cells. *Trends Mol. Med.* **18,** 348–359

47. Canalis, E., Mazziotti, G., Giustina, A., and Bilezikian, J. P. (2007) Glucocorticoid-induced osteoporosis: pathophysiology and therapy. *Osteoporos. Int.* **18,** 1319–1328

48. Zhang, M., Xuan, S., Bouxsein, M. L., von Stechow, D., Akeno, N., Faugere, M. C., Malluche, H., Zhao, G., Rosen, C. J., Efstratiadis, A., and Clemens, T. L. (2002) Osteoblast-specific knockout of the insulin-like growth factor (IGF) receptor gene reveals an essential role of IGF signaling in bone matrix mineralization. *J. Biol. Chem.* **277,** 44005–44012

49. Regan, J. N., Lim, J., Shi, Y., Joeng, K. S., Arbeit, J. M., Shohet, R. V., and Long, F. (2014) Up-regulation of glycolytic metabolism is required for HIF1α-driven bone formation. *Proc. Natl. Acad. Sci. U.S.A.* **111,** 8673–8678

50. Ohlsson, C., Mohan, S., Sjögren, K., Tivesten, A., Isgaard, J., Isaksson, O., Jansson, J. O., and Svensson, J. (2009) The role of liver-derived insulin-like growth factor-I. *Endocr. Rev.* **30,** 494–535

51. Shomento, S. H., Wan, C., Cao, X., Faugere, M. C., Bouxsein, M. L., Clemens, T. L., and Riddle, R. C. (2010) Hypoxia-inducible factors 1α and 2α

exert both distinct and overlapping functions in long bone development. *J. Cell Biochem.* **109,** 196 –204

52. Song, G., and Wang, L. (2008) Transcriptional mechanism for the paired miR-433 and miR-127 genes by nuclear receptors SHP and ERRγ. *Nucleic Acids Res.* **36,** 5727–5735

53. Jeong, B. C., Lee, Y. S., Bae, I. H., Lee, C. H., Shin, H. I., Ha, H. J., Franceschi, R. T., Choi, H. S., and Koh, J. T. (2010) The orphan nuclear receptor SHP is a positive regulator of osteoblastic bone formation. *J. Bone Miner. Res.* **25,** 262–274

54. Dufour, C. R., Levasseur, M. P., Pham, N. H., Eichner, L. J., Wilson, B. J., Charest-Marcotte, A., Duguay, D., Poirier-Héon, J. F., Cermakian, N., and Giguère, V. (2011) Genomic convergence among ERRα, PROX1, and BMAL1 in the control of metabolic clock outputs. *PLoS Genet.* **7,** e1002143

55. Villena, J. A., and Kralli, A. (2008) ERRα: a metabolic function for the oldest orphan. *Trends Endocrinol. Metab.* **19,** 269 –276

56. Möller-Levet, C. S., Archer, S. N., Bucca, G., Laing, E. E., Slak, A., Kabiljo, R., Lo, J. C., Santhi, N., von Schantz, M., Smith, C. P., and Dijk, D. J. (2013) Effects of insufficient sleep on circadian rhythmicity and expression amplitude of the human blood transcriptome. *Proc. Natl. Acad. Sci. U.S.A.* **110,** E1132–E1141

57. Golombek, D. A., Casiraghi, L. P., Agostino, P. V., Paladino, N., Duhart, J. M., Plano, S. A., and Chiesa, J. J. (2013) The times they're a-changing: effects of circadian desynchronization on physiology and disease. *J. Physiol. Paris* **107,** 310 –322

58. Schneider, C. A., Rasband, W. S., and Eliceiri, K. W. (2012) NIH Image to ImageJ: 25 years of image analysis. *Nat. Methods* **9,** 671– 675

Supplemental Materials

A.

GACGGCGCTAGGATCATCAAC<u>ACACCGAGGAGCCTAACCATCATGAT</u>CAAGTATTCTGGTC
ACAGAATAC<u>AACACACCGAGGAGCCTAACCATCATGAT</u>CAAGATGATCCTAGCGCCGTCC
GA

B.

GATATCGACGGCGCTAGGATCATCAAC<u>TCTACTCTTTCTAGAGCTGAGGTTGTGA</u>CAAGTA
TTCTGGTCACAGAATACAA<u>CTCTACTCTTTCTAGAGCTGAGGTTGTGA</u>CAAGATGATCCTAG
CGCCGTCATCGAT

C.

GACGGCGCTAGGATCATCAAC<u>ACACCGAGGAGCCTAACCATCATGAT</u>CAAGTATTCTGGTC
ACAGAATAC<u>AACACACCGAGGAGCCTAACCATCATGAT</u>CAAGATGATCCTAGCGCCGTCCa
ggttgttccaatgccaatctgtaaatacgagattcttaacgggttcaattcgcaactattggacaacaacacaaatggaccGACGG
CGCTAGGATCATCAAC<u>ACACCGAGGAGCCTAACCATCATGAT</u>CAAGTATTCTGGTCACAGA
ATAC<u>AACACACCGAGGAGCCTAACCATCATGAT</u>CAAGATGATCCTAGCGCCGTCGGCCGG
CCGTCGACCTGCAGTtttgaagaagagatccgctccagtaatggagaatattcttgatgtGACGGCGCTAGGATC
ATCAAC<u>ACACCGAGGAGCCTAACCATCATGAT</u>CAAGTATTCTGGTCACAGAATAC<u>AACACA
CCGAGGAGCCTAACCATCATGAT</u>CAAGATGATCCTAGCGCCGTCCGA

Supplemental Figure 1. Sequence of miR-433 decoy and non-targeting decoys used in vitro and in vivo.
(A) miR-433 tough decoy used in vitro, with miR-433 binding sites underlined (GenScript custom synthesis)
(B) Non-targeting tough decoy used in vitro. It contains C. elegans miR-67 binding sites, which are underlined (GenScript custom synthesis)
(C) Sequence of miR-433 decoy used for transgenic mouse: Three miR-433 tough decoys were assembled. DNA from the coding region of the C. elegans Cut3 gene was used as spacer between the repeats of miR-433 decoy, and is denoted by lower case letters. The miR-433 binding sites are underlined. The fragment was custom synthesized by GenScript.

Supplemental Table 1: Primer sequences used for qPCR analysis.	
Gene (mouse)	**Sequence**
18S (sense)	5'-GCGTGTGCCTACCCTACGCC -3'
18S (antisense)	5'-ACGCAAGCTTATGGCCCGCA-3'
Bmal1 (sense)	5'-AACCTTCCCGCAGCTAACAG -3'
Bmal1 (antisense)	5'-AGTCCTCTTTGGGCCACCTT -3'
Per2 (sense)	5'-AGAACGCGGATATGTTTGCTG-3'
Per2 (antisense)	5'-ATCTAAGCCGCTGCACACACT-3'
Hif1α (sense)	5'-ACCTTCATCGGAAACTCCAAAG -3'
Hif1α (antisense)	5'-ACTGTTAGGCTCAGGTGAACT-3'
Nr3c1 (sense)	5'-GTGAGTTCTCCTCCGTCCAG -3'
Nr3c1 (antisense)	5'-TGCAATCATTTCTTCCAGCA-3'
Runx2 (sense)	5'-CCTCTGGCCTTCCTCTCTCAGT -3'
Runx2 (antisense)	5'-GCCACTCTGGCTTTGGGAAGAG -3'
Igf1(sense)	5'-CACACTGACATGCCCAAGAC -3'
Igf1 (antisense)	5'-GGGAGGCTCCTCCTACATTC -3'
GFP (sense)	5'-GTGAGCAAGGGCGAGGAGCTGTTC -3'
GFP (antisense)	5'-GTAGGTCAGGGTGGTCACGAGGG -3'
GRα (sense)	5'-AAAGAGCTAGGAAAAGCCCATTGTC-3'
GRα (antisense)	5'-TCAGCTAACATCTCTGGGAATTCA -3'
GRβ (sense)	5'-AAAGAGCTAGGAAAAGCCCATTGTC-3'
GRβ (antisense)	5'-CTGTCTTTGGGCTTTTGAGATAGG -3'
Dusp1 (sense)	5'-CAGCTGCTGCAGTTTGAGTC -3'
Dusp1 (antisense)	5'-GGGATGGAAACAGGGAAGTT -3'

MicroRNA-433 Dampens Glucocorticoid Receptor Signaling, Impacting Circadian Rhythm and Osteoblastic Gene Expression

Spenser S. Smith, Neha S. Dole, Tiziana Franceschetti, Henry C. Hrdlicka and Anne M. Delany

Access the most updated version of this article at doi: 10.1074/jbc.M116.737890

Alerts:
- When this article is cited
- When a correction for this article is posted

Click here to choose from all of JBC's e-mail alerts

Supplemental material:
http://www.jbc.org/content/suppl/2016/08/22/M116.737890.DC1.html

This article cites 58 references, 16 of which can be accessed free at
http://www.jbc.org/content/291/41/21717.full.html#ref-list-1